

# Deflection in higher dimensional spacetime and asymptotically non-Minkowski spacetime

Jinhong He,<sup>\*</sup> Qianchuan Wang,<sup>\*</sup> Qiyue Hu, and Li Feng

*School of Physics and Technology, Wuhan University, Wuhan, 430072, China*

Junji Jia<sup>†</sup>

*Center for Astrophysics & MOE Key Laboratory of Artificial Micro- and Nano-structures,*

*School of Physics and Technology, Wuhan University, Wuhan, 430072, China*

(Dated: October 4, 2022)

## Abstract

Using a perturbative technique, in this work we study the deflection of null and timelike signals in the extended Einstein-Maxwell spacetime, the Born-Infeld gravity and the charged Ellis-Bronnikov (CEB) spacetime in the weak field limit. The deflection angles are found to take a (quasi-)series form of the impact parameter, and automatically takes into account the finite distance effect of the source and observer. The method is also applied to find the deflections in CEB spacetime with arbitrary dimension. It's shown that to the leading non-trivial order the deflection in an  $n$ -dimensional spacetime is of the order  $\mathcal{O}(M/b)^{n-3}$ . We then extended the method to spacetimes that are asymptotically non-Minkowski and studied the deflection in a nonlinear electro-dynamical scalar theory. The deflection angle in asymptotically non-Minkowski spacetimes at the trivial order is found to be not  $\pi$  anymore. In all these cases, the perturbative deflection angles are shown to agree with numerical results extremely well. The effects of some nontrivial spacetime parameters as well as the signal velocity on the deflection angles are analyzed.

Keywords: deflection angle, perturbative method, timelike signal, high dimensional spacetime

---

<sup>\*</sup>These authors contributed equally to this work.

<sup>†</sup>Corresponding author: junjijia@whu.edu.cn

## I. INTRODUCTION

The deflection and gravitational lensing (GL) of light rays are important tools in astronomy. The former historically contributed significantly to the acceptance of general relativity (GR) by scientists [1]. And the latter is being used to find exoplanets [2, 3], to measure the mass distribution of galaxies and their clusters [4, 5], and to test theories beyond GR [6, 7]. In recent years, with the observation of gravitational wave (GW) [8] and the black hole shadow [9–11], the deflection and GL of GW, as well as the deflection and GL of light rays in the strong field limit, have drawn enormous amount of attention.

On the other hand, after the discovery of cosmic rays [12] and the SN 1987A neutrinos [13, 14], especially after the confirmation of the extrasolar origin of the former [15, 16] and the nonzero mass of the latter [17, 18], people become aware that massive signals such as cosmic rays and neutrinos from various sources can also experience gravitational deflection and be messengers of GL. One particularly encouraging progress in this direction is the discovery of GLed supernovas in recent years [19, 20].

To theoretically investigate the deflection of these signals, recently two methods have been intensively used. One is to use the Gauss-Bonnet theorem method [21–23], which has been developed to handle both null and timelike signals [23–26], and to take into account the finite distance effect of the source and detector [27–29], as well as the electromagnetic force [26, 29, 30]. The other method is the perturbative method developed by some authors of this paper. The method can also calculate the deflection of both null and timelike signals [31] and has been extended to include the finite distance effect [32] and the extra kind of force [33, 34] too. Moreover, the perturbative method can be used in arbitrary stationary and axisymmetric spacetimes [31, 32], as well as in the strong field limit [35].

There are two folds of motivations of this work. The first is to apply the perturbative method previously developed to other interesting spacetimes, namely the extended Einstein-Maxwell spacetime [36], the Born-Infeld gravity [37] and the charged Ellis-Bronnikov (CEB) spacetime [38], to study the effect of the various spacetime parameters on the deflection of signals in these spacetimes. The second motivation is to test whether the perturbative method can be extended to treat rare spacetimes, particularly the higher dimensional ones and asymptotically non-Minkowski ones. As we will see, it turns out the extension is actually quite simple and we will apply it to the higher dimensional CEB spacetime and a nonlinear

electrodynamical scalar (NES) theory.

The paper is organized as follows. In Sec. II we recap the perturbative method that was previously developed. In Sec. III we apply the method to three spacetimes that are asymptotically Minkowski, and study the effects of the spacetime parameters on the deflection of both null and timelike signals. We emphasize that to our knowledge, the deflections in these spacetimes in the weak field limit were not studied before. Moreover, in Subsec. III C, we also use the perturbative method to study the deflection in the higher dimensional CEB spacetime. In Sec. IV, the perturbative method is extended to the asymptotically non-Minkowski case and used to study the NES theory. We also point out a prominent feature of the deflection angle in this kind of spacetimes. We conclude the work with a short discussion in Sec. V. Throughout this work, we adopt the natural unit system  $G = c = 1$  and the most plus metric convention.

## II. THE PERTURBATIVE METHOD

The perturbative method to calculate the deflection angle in the static and spherically symmetric spacetimes in the weak field limit was initiated in Ref. [31] and further formalized in Ref. [32]. There, the metric functions were assumed to allow asymptotic expansions into integer power series of the radius. In this section, we will first recap the main procedure of this method and then extend it to asymptotically non-Minkowski metrics in Sec. IV.

Static and spherically symmetric spacetimes can always be described by the line element

$$ds^2 = -A(r)dt^2 + B(r)dr^2 + C(r)(d\theta^2 + \sin^2\theta d\phi^2), \quad (1)$$

where  $(t, r, \theta, \phi)$  are the coordinates and  $A(r)$ ,  $B(r)$  and  $C(r)$  are the metric functions of  $r$  only. The asymptotic flatness of the spacetime often allows the following asymptotic expansion of the metric functions

$$A(r) = 1 + \sum_{n=1} \frac{a_n}{r^n}, \quad B(r) = 1 + \sum_{n=1} \frac{b_n}{r^n}, \quad \frac{C(r)}{r^2} = 1 + \sum_{n=1} \frac{c_n}{r^n}, \quad (2)$$

where  $a_n$ ,  $b_n$  and  $c_n$  are finite constants. Although locally we can always set  $C(r) = r^2$ , there are occasions that  $C(r)$  is transformed to other forms and therefore we will keep its general form as in (2) for now. The geodesic equations associated with a test particle in this

spacetime can be readily obtained as

$$\dot{t} = \frac{E}{A(r)}, \quad (3a)$$

$$\dot{\phi} = \frac{L}{C(r)}, \quad (3b)$$

$$\dot{r}^2 = \frac{1}{B(r)} \left( \kappa - \frac{E^2}{A(r)} + \frac{L^2}{C(r)} \right), \quad (3c)$$

where the dot stands for the derivative with respect to the affine parameter.  $L$  and  $E$  are respectively the conserved angular momentum and energy per unit mass of the signal, and  $\kappa = 0$  and  $1$  respectively for null and timelike signals.

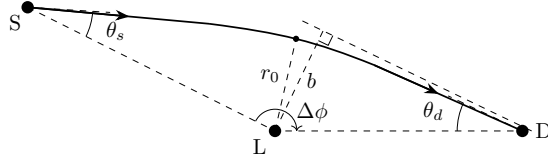


FIG. 1: The trajectory from the source S at radius  $r_s$  to the detector D at  $r_d$ , passing by the lens L. The impact parameter and closest approach are marked as  $b$  and  $r_0$  respectively.

From these equations, one can express the deflection angle  $\Delta\phi$  from the source at coordinate  $(r_s, \phi_s)$  to the detector at  $(r_d, \phi_d)$  (see Fig. 1) as [32, 39]

$$\Delta\phi = \left[ \int_{r_0}^{r_s} + \int_{r_0}^{r_d} \right] \sqrt{\frac{B}{C}} \frac{L}{\sqrt{(E^2/A - \kappa)C - L^2}} dr, \quad (4)$$

where  $r_0$  is the closest approach of the trajectory and can be solved from the condition  $\dot{r}|_{r=r_0} = 0$ . Using Eq. (3c), this condition can also establish a relation between  $L$  and  $r_0$

$$L = \sqrt{[E^2 - \kappa A(r_0)]C(r_0)/A(r_0)}. \quad (5)$$

In an asymptotically flat spacetime,  $L$  and  $E$  can also be expressed as

$$L = |\mathbf{r} \times \mathbf{p}| = \frac{v}{\sqrt{1-v^2}} b, \quad E = \frac{1}{\sqrt{1-v^2}}, \quad (6)$$

where  $v$  is the signal velocity at infinity and  $b$  is the impact parameter. Solving  $b$  from Eq. (6) and using Eq. (5), we have

$$\frac{1}{b} = \frac{\sqrt{E^2 - \kappa}}{\sqrt{E^2 - \kappa A(r_0)}} \sqrt{\frac{A(r_0)}{C(r_0)}} \quad (7)$$

$$\equiv p\left(\frac{1}{r_0}\right) \quad (8)$$

where in the last step the right-hand side of Eq. (7) is defined as a function  $p$  of  $1/r_0$ . For later purpose, we will denote the inverse function of  $p(x)$  as  $q(x)$ . We point out that as long as the metric functions are known, both functions  $p(x)$  and  $q(x)$  can be known too (at least perturbatively).

To calculate  $\Delta\phi$  in (4), in Ref. [32, 39] we proposed the change of variable from  $r$  to  $u$  using the relation

$$r = 1/q\left(\frac{u}{b}\right). \quad (9)$$

Substituting Eq. (9) into Eq. (4), it is not too difficult to verify that it is transformed to

$$\Delta\phi = \left[ \int_{\sin\theta_s}^1 + \int_{\sin\theta_d}^1 \right] y\left(\frac{u}{b}\right) \frac{du}{\sqrt{1-u^2}}, \quad (10)$$

where

$$y\left(\frac{u}{b}\right) = \sqrt{\frac{B(1/q)}{C(1/q)}} \frac{1}{p'(q)q^2} \frac{u}{b}, \quad (11)$$

and

$$\theta_s = \arcsin\left[b \cdot p\left(\frac{1}{r_s}\right)\right], \quad \theta_d = \arcsin\left[b \cdot p\left(\frac{1}{r_d}\right)\right] \quad (12)$$

are actually the apparent angles of the signal at the source and detector respectively.

In the weak field limit,  $y(u/b)$  in Eq. (10) can be expanded into a power series of  $u/b$ , i.e.,

$$y\left(\frac{u}{b}\right) = \sum_{n=0}^{\infty} y_n \left(\frac{u}{b}\right)^n, \quad (13)$$

where  $y_n$  can be expressed in terms of coefficients in the asymptotic expansions (2) of the metric. The first few of them are

$$y_0 = 1, \quad (14a)$$

$$y_1 = \frac{b_1}{2} - \frac{a_1}{2v^2}, \quad (14b)$$

$$y_2 = \frac{4(c_2 + b_2) - (c_1 - b_1)^2}{8} + \frac{a_1(2a_1 - c_1 - b_1) - 2a_2}{2v^2}. \quad (14c)$$

Higher order coefficients are also easily obtained and can be seen in Appendices of Ref. [32, 39]. From Eq. (14), it is seen that for the order  $n$  coefficient  $y_n$ , only the metric expansion coefficients up to order  $n$ , i.e.  $a_n$ ,  $b_n$  and  $c_n$ , contribute.

Substituting Eq. (13) into Eq. (10),  $\Delta\phi$  becomes a sum containing a series of integrals of the form

$$I_n(\theta_s, \theta_d) = \left[ \int_{\sin\theta_s}^1 + \int_{\sin\theta_d}^1 \right] \frac{u^n}{\sqrt{1-u^2}} du, \quad (n = 0, 1, \dots). \quad (15)$$

Integrals of this type can always be carried out and their results are present in Eq. (A2) in Appendix A. Therefore, the above change of variables and series expansion guarantee that we can obtain the following quasi-inverse power series form of the deflection angle

$$\Delta\phi = \sum_{n=0}^{\infty} y_n \frac{I_n(\theta_s, \theta_d)}{b^n}. \quad (16)$$

In the large  $r_s$  and  $r_d$  limit, from Eq. (12) we see that  $\theta_s, \theta_d$  are small and then one can expand  $I_n(\theta_s, \theta_d)$  as series of  $b/r_s$  and  $b/r_d$  using Eq. (A4). After this,  $\Delta\phi$  in Eq. (16) becomes pure series of  $(M/b)$  and  $(b/r_{s,d})$ . To the first few orders, it is

$$\begin{aligned} \Delta\phi = & \sum_{i=s,d} \frac{\pi}{2} + \frac{1}{2b} \left( b_1 - \frac{a_1}{v^2} \right) - \frac{\pi}{32b^2} \left\{ (b_1 - c_1)^2 - 4(b_2 + c_2) + \frac{8}{v^2} \left[ \frac{a_1(b_1 + c_1)}{2} - a_1^2 + a_2 \right] \right\} \\ & + \frac{1}{b^3} \left\{ \frac{1}{24} [-2b_1^2 c_1 - 4b_1(b_2 - 2c_2) + 8(b_2 c_1 + b_3 + 2c_3) + b_1^3] \right. \\ & + \frac{1}{8v^2} [4a_1^2(b_1 + 2c_1) + a_1(16a_2 - 4b_1 c_1 - 4(b_2 + 2c_2) + b_1^2) - 4a_2(b_1 + 2c_1) - 8a_1^3 - 8a_3] \\ & \left. + \frac{1}{8v^4} [a_1(a_1(b_1 + 2c_1) - 4a_1^2 + 4a_2)] + \frac{a_1^3}{24v^6} \right\} \\ & - \frac{b}{r_i} + \frac{b}{4r_i^2} \left( -b_1 + 2c_1 - \frac{a_1}{v^2} \right) - \frac{b^3}{6r_i^3} + \mathcal{O} \left[ \left( \frac{M}{b} \right)^4, \left( \frac{b}{r_i} \right)^4 \right]. \quad (17) \end{aligned}$$

In the infinite  $r_s, r_d$  limit, this becomes

$$\Delta\phi = \pi + \left( b_1 - \frac{a_1}{v^2} \right) \frac{1}{b} + \left( \frac{4(b_2 + c_2) - (b_1 - c_1)^2}{4} + \frac{a_1(2a_1 - b_1 - c_1) - 2a_2}{v^2} \right) \frac{\pi}{4b^2} + \mathcal{O} \left( \frac{1}{b} \right)^3. \quad (18)$$

### III. APPLICATIONS TO PARTICULAR SPACETIMES

In this section, we will directly apply the above method to some known spacetimes to check the validity of Eq. (16), and more importantly, to reveal how any parameters of the spacetime and the particle velocity will affect the deflections.

### A. Extended Einstein-Maxwell Spacetime

The extended Einstein-Maxwell theory describes a charged spacetime without the central singularity [36]. Its line element is given by Eq. (1) with the following metric functions

$$A(r) = \frac{1}{B(r)} = \frac{r^4(r^2 - 2Mr + Q^2) + \alpha Q^2(3r^2 + 2\alpha)}{r^6 + \alpha Q^2(r^2 + 2\alpha)}, \quad C(r) = r^2. \quad (19)$$

Here  $M$  and  $Q$  are respectively the spacetime mass and charge, while  $\alpha$  is a scale parameter with a length square dimension. Expanding these metric functions asymptotically, we have up to the fourth order

$$A(r) = 1 - \frac{2M}{r} + \frac{Q^2}{r^2} + \frac{2Q^2\alpha}{r^4} + \mathcal{O}(r)^{-5}, \quad (20a)$$

$$B(r) = 1 + \frac{2M}{r} + \frac{4M^2 - Q^2}{r^2} + \frac{8M^3 - 4MQ^2}{r^3} + \frac{16M^4 - 12M^2Q^2 + Q^4 - 2Q^2\alpha}{r^4} + \mathcal{O}(r)^{-5}, \quad (20b)$$

$$\frac{C(r)}{r^2} = 1. \quad (20c)$$

Reading off the coefficients  $a_i$ ,  $b_i$  and  $c_i$  and substituting into Eq. (14), we get the coefficients  $y_n$  up to the fourth order in the deflection angle  $\Delta\phi_E$  in this spacetime, as

$$y_{E,0} = 1, \quad (21a)$$

$$y_{E,1} = M \left( 1 + \frac{1}{v^2} \right), \quad (21b)$$

$$y_{E,2} = M^2 \left( \frac{3}{2} + \frac{6}{v^2} \right) - Q^2 \left( \frac{1}{2} + \frac{1}{v^2} \right), \quad (21c)$$

$$y_{E,3} = M^3 \left( \frac{5}{2} + \frac{45}{2v^2} + \frac{15}{2v^4} - \frac{1}{2v^6} \right) - MQ^2 \left( \frac{3}{2} + \frac{9}{v^2} + \frac{3}{2v^4} \right), \quad (21d)$$

$$y_{E,4} = M^4 \left( \frac{35}{8} + \frac{70}{v^2} + \frac{70}{v^4} \right) - M^2Q^2 \left( \frac{15}{4} + \frac{45}{v^2} + \frac{30}{v^4} \right) + Q^4 \left( \frac{3}{8} + \frac{3}{v^2} + \frac{1}{v^4} \right) - Q^2\alpha \left( 1 + \frac{4}{v^2} \right). \quad (21e)$$

Substituting these into Eq. (16),  $\Delta\phi_E$  is found to be

$$\Delta\phi_E = \sum_{n=0}^{\infty} y_{E,n} \frac{I_n(\theta_s, \theta_d)}{b^n}, \quad (22)$$

where  $I_n(\theta_s, \theta_d)$  ( $n = 0, 1, \dots$ ) are given in Eq. (A2). Note that higher than the fourth order results for the coefficients are easily obtainable too but not shown here for their excessive length.

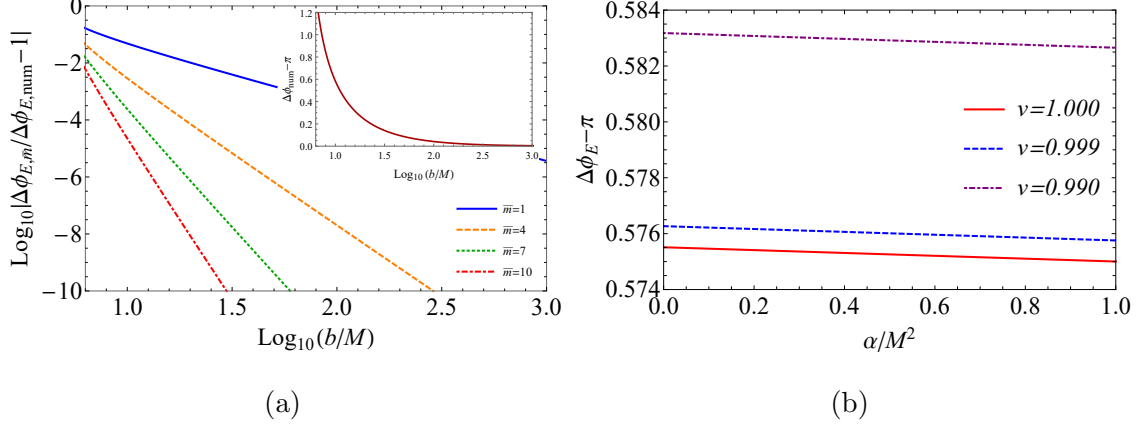


FIG. 2: (a) Difference between the perturbative  $\Delta\phi_{E,\bar{m}}$  and the numerical result  $\Delta\phi_{E,\text{num}}$  as a function of  $b/M$  from 7 to  $10^3$ . The inset shows the deflection angle itself for this range of  $b$ . Other parameters used are  $Q = M/2$ ,  $v = 1 - 10^{-2}$ ,  $r_s = r_d = 10^6 M$  and  $\alpha = 10^{-2} M^2$ . (b)  $\Delta\phi_E - \pi$  as a function of  $\alpha$  for  $b = 10M$  and three values of  $v = 1, 0.999, 0.990$ . Other parameters are the same as in (a).

To check the correctness of  $\Delta\phi_E$ , we define a truncated  $\Delta\phi_{E,\bar{m}}$  as the sum of up to the  $\bar{m}$ -th order

$$\Delta\phi_{E,\bar{m}} = \sum_{n=0}^{\bar{m}} y_n \frac{I_n(\theta_s, \theta_d)}{b^n} \quad (\bar{m} = 1, 2, \dots), \quad (23)$$

and then in Fig. 2 (a) we plot the difference between  $\Delta\phi_{E,\bar{m}}$  and the numerical integration result  $\Delta\phi_{E,\text{num}}$  of the original Eq. (4) using the metric (19). As long as the numerical integration is done with high enough precision, its result can be thought as the true deflection of the trajectory and all perturbative results can be compared against it. We then see from the figure that for any fixed impact parameter  $b$ , as the truncation order increases, the perturbative result approaches the true value exponentially. Moreover, we see that as  $b$  increases,  $\Delta\phi_E$  decreases (see the inset) as dictated by the quasi-inverse power series of the form (22), and the accuracy for each  $\Delta\phi_{E,\bar{m}}$  also increases. At about  $b = 10^3 M$ , the relative difference between  $\Delta\phi_{E,\bar{4}}$  and  $\Delta\phi_{E,\text{num}}$  is less than  $10^{-10}$ . Note that the relative difference between  $\Delta\phi_{E,\bar{10}}$  and  $\Delta\phi_{E,\text{num}}$  at impact parameter as small as  $b = 10M$  is still quite small, while the  $\Delta\phi_E$  itself at this point is already 0.6, not truly a weak deflection anymore. All the above features and comparison show that the  $\Delta\phi_E$  found in Eq. (22) can approximate the true deflection angle to very high precision as long as the truncation order is high enough.

With the correctness of Eq. (22) confirmed, we can now use it to study the effects of

the scale parameter  $\alpha$  and the kinetic variable  $v$  on the deflection angle. Here we will concentrate on the effect of the parameter  $\alpha$  but not charge  $Q$  because the latter was well studied in Reissner-Nordström (RN) spacetime [40]. Eq. (21e) shows that  $\alpha$  only appear from the fourth order  $y_4$  in  $\Delta\phi_E$  and therefore it is expected that in general, its effect to the deflection will be very small as long as its size does not exceed unity, i.e.,  $\alpha \lesssim \mathcal{O}(M^2)$ . Moreover, it is also clear that the smaller the impact parameter  $b$ , the larger the effect of  $\alpha$  on the overall size of  $\Delta\phi$ . In Fig. 2 (b) we plot the variation of  $\Delta\phi_E$  as a function of  $\alpha$  for  $b = 10M$ . It is clear that as  $\alpha$  increases, the deflection angle decreases monotonically. This is consistent with Eq. (21e) in which the term involving  $\alpha$  has a negative sign. It is also seen that the larger the velocity  $v$ , the smaller the deflection, which is also in accord with the intuition from Newtonian mechanics.

## B. The Born-Infeld gravity

The Born-Infeld gravity describes gravity coupled with Born-Infeld electrodynamics [37]. Its metric functions for a special type are given by [37]

$$A(r) = \left(1 - \frac{4\eta Q^2}{(r^2 + \sqrt{r^4 + 4\eta Q^2})^2}\right) \left(1 - \frac{2\sqrt{2}M}{\sqrt{r^2 + \sqrt{r^4 + 4\eta Q^2}}} + \frac{2Q^2}{r^2 + \sqrt{r^4 + 4\eta Q^2}}\right), \quad (24a)$$

$$B(r) = \frac{2r^2}{(r^2 + \sqrt{r^4 + 4\eta Q^2})A(r)}, \quad (24b)$$

$$\frac{C(r)}{r^2} = 1. \quad (24c)$$

Here  $M$  and  $Q$  are respectively the mass and charge of the spacetime and  $\eta > 0$  characterizes the relative scale of the electromagnetic and gravity sectors of the theory. When  $\eta = 0$ , this reduces to the classical RN spacetime. Therefore,  $\eta$  can be regarded as a parameter that measures the deviation of the gravity from the RN spacetime. Only when  $|Q| \leq M$  and  $0 < \eta < \eta_+$  where  $\eta_{\pm} = M^4 \left(1 \pm \sqrt{1 - Q^2/M^2}\right)^4 / Q^2$  will this metric describe a BH spacetime [41–45]. When  $0 < \eta < \eta_-$ , the BH has two event horizons located at  $r_{H\pm}$

$$r_{H\pm} = \frac{\sqrt{\left(M \pm \sqrt{M^2 - Q^2}\right)^4 - \eta Q^2}}{M \pm \sqrt{M^2 - Q^2}} \quad (25)$$

and when  $\eta_- < \eta < \eta_+$  only one horizon at  $r_{H+}$  survives.

Expanding metric functions (24c) at large  $r$ , we have

$$A(r) = 1 - \frac{2M}{r} + \frac{Q^2}{r^2} + \frac{\eta Q^2}{r^4} + \mathcal{O}(r)^{-5}, \quad (26a)$$

$$B(r) = 1 + \frac{2M}{r} + \frac{4M^2 - Q^2}{r^2} + \frac{8M^3 - 4MQ^2}{r^3} + \frac{16M^4 - 12M^2Q^2 + Q^4 - 2\eta Q^2}{r^4} + \mathcal{O}(r)^{-5}, \quad (26b)$$

$$\frac{C(r)}{r^2} = 1, \quad (26c)$$

from which their first few coefficients  $a_i$ ,  $b_i$  and  $c_i$  are easily read off. Substituting these into Eq. (14), the coefficients  $y_{B,n}$  in this case are found to be

$$y_{B,0} = 1, \quad (27a)$$

$$y_{B,1} = M \left( 1 + \frac{1}{v^2} \right), \quad (27b)$$

$$y_{B,2} = M^2 \left( \frac{3}{2} + \frac{6}{v^2} \right) - Q^2 \left( \frac{1}{2} + \frac{1}{v^2} \right), \quad (27c)$$

$$y_{B,3} = M^2 \left( \frac{5}{2} + \frac{45}{2v^2} + \frac{15}{2v^2} - \frac{1}{2v^6} \right) - Q^2 \left( \frac{3}{2} + \frac{9}{v^2} + \frac{3}{2v^4} \right), \quad (27d)$$

$$y_{B,4} = M^4 \left( \frac{35}{8} + \frac{70}{v^2} + \frac{70}{v^4} \right) - M^2 Q^2 \left( \frac{15}{4} + \frac{45}{v^2} + \frac{30}{v^4} \right) + Q^4 \left( \frac{3}{8} + \frac{3}{v^2} + \frac{1}{v^4} \right) - Q^2 \eta \left( 1 + \frac{2}{v^2} \right). \quad (27e)$$

Substituting these into Eq. (16), the deflection in this Born-Infeld gravity becomes

$$\Delta\phi_B = \sum_{n=0}^{\infty} y_{B,n} \frac{I_n(\theta_s, \theta_d)}{b^n}. \quad (28)$$

For null signals except photons, we can easily take the  $v = 1$  limit in Eq. (27) to obtain its deflection angle. Similar to the extended Einstein-Maxwell case in Eq. (21e), the parameter  $\eta$  controlling the deviation from the RN spacetime also appears from the fourth order in Eq. (27e). We will see in Fig. 3 that this similarity leads to quantitatively similar effect of the parameter  $\eta$  on the deflection angle  $\Delta\phi_B$  as that of the parameter  $\alpha$  on the deflection angle  $\Delta\phi_E$  in the extended Einstein-Maxwell gravity.

In Fig. 3 (a), we plot the truncated deflection angles

$$\Delta\phi_{B,\bar{m}} = \sum_{n=0}^{\bar{m}} y_{B,n} \frac{I_n(\theta_s, \theta_d)}{b^n}, \quad (\bar{m} = 1, 2, \dots) \quad (29)$$

to different orders as functions of the impact parameter. The deflection angle  $\Delta\phi_{B,\text{num}}$  obtained by directly numerically integrating Eq. (4) is compared with the truncated  $\Delta\phi_{B,\bar{m}}$ . It is seen that similar to the case of the extended Einstein-Maxwell spacetime, as the truncation order increases, the perturbative result approaches the numerical value for all  $b$ . Moreover, the larger the  $b$  is, the smaller the difference between  $\Delta\phi_{B,\bar{m}}$  and  $\Delta\phi_{B,\text{num}}$ . When the truncation order  $\bar{m} = 10$ ,  $\Delta\phi_{B,10}$  is still a good approximation of the angle even for  $b = 10M$ , at which point  $\Delta\phi_B$  is also about 0.6 and the gravity is not that weak anymore.

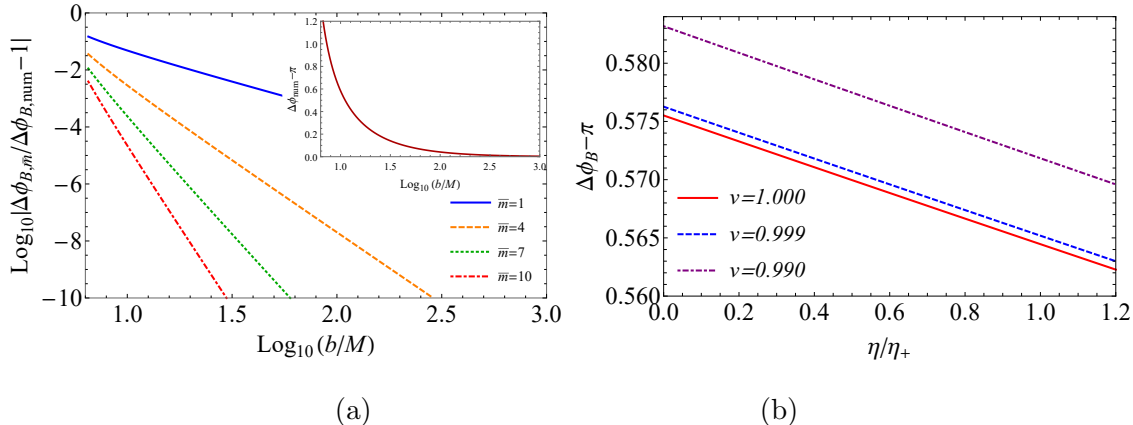


FIG. 3: (a) Difference between the perturbative  $\Delta\phi_{B,\bar{m}}$  and the numerical result  $\Delta\phi_{B,\text{num}}$  as a function of  $b/M$  from 7 to  $10^3$ . The inset shows the deflection angle itself for this range of  $b$ . Other parameters used are  $Q = M/2$ ,  $v = 1 - 10^{-2}$ ,  $r_s = r_d = 10^6 M$  and  $\eta = M/5$ . (b)  $\Delta\phi_B - \pi$  as a function of  $\eta/M$  for  $b = 10M$  and three values of  $v = 1, 0.999, 0.990$ . Other parameters are the same as in (a).

With the perturbative result checked, we can now use it to study the effect of spacetime parameter  $\eta$  on the deflection angle. In Fig. 3 (b), we plotted  $\Delta\phi_B$  as a function of  $\eta$  from 0 to  $1.2\eta_+$  for several  $v$ . It is seen that for the chosen values of other parameters,  $\eta$  affects the deflection angle only by about 0.01 which is quite small comparing to the absolute value of the deflection angle itself. The effect of  $\eta$  in this spacetime then is also much weaker than that of the charge  $Q$  from 0 to  $M$ , as was revealed in Ref. [40].

For photons, due to the influence of nonlinear electrodynamics, their motion can be regarded as moving along the geodesic line in an effective spacetime [37]. The metric functions of this spacetime is given by

$$A_{\text{eff}}(\bar{r}) = \left(1 + \frac{\eta Q^2}{\bar{r}^4}\right) \left(1 - \frac{2M}{\bar{r}} + \frac{Q^2}{\bar{r}^2}\right), \quad (30a)$$

$$B_{\text{eff}}(\bar{r}) = \frac{1 + \frac{\eta Q^2}{\bar{r}^4}}{1 - \frac{2M}{\bar{r}} + \frac{Q^2}{\bar{r}^2}}, \quad (30b)$$

$$C_{\text{eff}}(\bar{r}) = \frac{\bar{r}^2 \left(1 + \frac{\eta Q^2}{\bar{r}^4}\right)^2}{1 - \frac{\eta Q^2}{\bar{r}^4}}, \quad (30c)$$

where  $\bar{r}$  is related to  $r$  by

$$\frac{\bar{r}^2 \left(1 + \frac{\eta Q^2}{\bar{r}^4}\right)^2}{1 - \frac{\eta Q^2}{\bar{r}^4}} = r^2. \quad (31)$$

Clearly, the weak field limit of large  $r$  is also the large  $\bar{r}$  limit.

To compute the deflection angle of a photon in this metric, we first note that metric (30) has a conformal factor  $\left(1 + \frac{\eta Q^2}{\bar{r}^4}\right)$  which will not affect the computation of photon's deflection angle (this can be recognized from Eq. (4)). Therefore, we can remove this factor and deal with the reduced metric of the form

$$A_{\text{red}}(\bar{r}) = \frac{1}{B_{\text{red}}(\bar{r})} = 1 - \frac{2M}{\bar{r}} + \frac{Q^2}{\bar{r}^2}, \quad C_{\text{red}}(\bar{r}) = \frac{\bar{r}^2 \left(1 + \frac{\eta Q^2}{\bar{r}^4}\right)}{1 - \frac{\eta Q^2}{\bar{r}^4}}. \quad (32)$$

To use the perturbative method for this metric, we expand it at large  $\bar{r}$

$$A_{\text{red}}(\bar{r}) = 1 - \frac{2M}{\bar{r}} + \frac{Q^2}{\bar{r}^2}, \quad (33a)$$

$$B_{\text{red}}(\bar{r}) = 1 + \frac{2M}{\bar{r}} + \frac{4M^2 - Q^2}{\bar{r}^2} + \frac{8M^3 - 4MQ^2}{\bar{r}^3} + \frac{16M^4 - 12M^2Q^2 + Q^4}{\bar{r}^4} + \mathcal{O}(\bar{r})^{-5}, \quad (33b)$$

$$\frac{C_{\text{red}}(\bar{r})}{\bar{r}^2} = 1 + \frac{2\eta Q^2}{\bar{r}^4} + \mathcal{O}(\bar{r})^{-5}. \quad (33c)$$

Substituting these into Eq. (14), the first few coefficients in the deflection angle (16) in this case are found to be

$$y'_{B,0} = 1, \quad (34a)$$

$$y'_{B,1} = 2M, \quad (34b)$$

$$y'_{B,2} = \frac{15M^3}{2} - \frac{3Q^2}{2}, \quad (34c)$$

$$y'_{B,3} = 32M^3 - 12MQ^2, \quad (34d)$$

$$y'_{B,4} = \frac{1155M^4}{8} - \frac{315M^2Q^2}{4} + \frac{35Q^4}{8} + 3\eta Q^2. \quad (34e)$$

Comparing to the  $v \rightarrow 1$  limit of the coefficients (27) for other null signals (such as gravitational wavelets), we find that there is only one difference in the sign of  $\eta$  in Eqs. (27e) and

(34e). A comparison in even high orders  $y_{B,n}$  and  $y'_{B,n}$  ( $n \geq 5$ ) shows that their difference also only appear in the sign of  $\eta$ . Therefore, we can conclude that from the asymptotic deflection angle point of view, the nonlinear parameter  $\eta$  influences photon and other null signals with different signs. Note however, this does not mean the deflection angles change their signs because the effect of  $\eta$  is only at the fourth order and above.

### C. Charged Ellis-Bronnikov spacetime

The charged Ellis-Bronnikov spacetime is the charged version of the Ellis-Bronnikov solution for the Einstein-Maxwell-(phantom)-dilaton theory. The metric functions of this spacetime are [38]

$$A(r) = e^{-2\beta U} W^{2a_c^2/(a^2 - a_c^2)}, \quad (35a)$$

$$B(r) = \left[ e^{2\beta U} W^{-2a_c^2/(a^2 - a_c^2)} V \right]^{1/(n-3)} / V, \quad (35b)$$

$$C(r) = \left[ e^{2\beta U} W^{-2a_c^2/(a^2 - a_c^2)} V \right]^{1/(n-3)} r^2, \quad (35c)$$

where  $n$  is the dimension of the spacetime and

$$U = \arctan \left( \frac{M}{2r^{n-3}} \right), \quad W = \frac{1 + q^2(a^2 - a_c^2)e^{2\beta_{\pm}U}}{1 + q^2(a^2 - a_c^2)}, \quad V = 1 + \frac{M^2}{4r^{2(n-3)}}, \quad (36a)$$

$$a_c = \sqrt{\frac{2(n-3)}{n-2}}, \quad \beta_{\pm} \equiv \pm \frac{a}{a_c} \sqrt{1 + \beta^2} - \beta. \quad (36b)$$

Here  $q$  is the electric charge of the spacetime,  $a$  is the dilaton coupling constant, and  $M$ ,  $\beta$  are parameters about the dilaton field in the Einstein-Maxwell-dilaton action. Note there is an equivalence between the solutions with parameters  $(M, a, \beta)$  and  $(-M, -a, -\beta)$ . Therefore we can concentrate on the case  $M > 0$  but keep two branches of  $\beta_{\pm}$ . And for simplicity, we will set  $n = 4$  first so that  $a_c = 1$  and study the general  $n$  case later. This charged Ellis-Bronnikov spacetime with certain ranges of the parameters describes a traversable wormhole bridging two asymptotically flat regions. In this work, we will focus on the range  $a > a_c = 1$ , which allows the existence of such wormhole.

The metric functions (35) can be expanded for large  $r$  to find their series forms

$$A(r) = 1 - 2Y \frac{M}{r} + (X^2 + 2Y^2) \frac{M^2}{r^2} + \left( \frac{Z}{3} X^3 - 2X^2Y - \frac{4}{3} Y^3 + \frac{Y}{6} \right) \frac{M^2}{r^3} + \mathcal{O}(r)^{-4}, \quad (37a)$$

$$B(r) = 1 + 2Y \frac{M}{r} + (-X^2 + 2Y^2) \frac{M^2}{r^2} + \left( \frac{Z}{3} X^3 - 2X^2Y + \frac{4}{3} Y^3 - \frac{Y}{6} \right) \frac{M^2}{r^3} + \mathcal{O}(r)^{-4}, \quad (37b)$$

$$\frac{C(r)}{r^2} = 1 + 2Y \frac{M}{r} + \left( -X^2 + 2Y^2 + \frac{1}{4} \right) \frac{M^2}{r^2} + \left( \frac{Z}{3} X^3 - 2X^2Y + \frac{4}{3} Y^3 + \frac{Y}{3} \right) \frac{M^2}{r^3} + \mathcal{O}(r)^{-4}, \quad (37c)$$

where to simplify the notation we have defined  $X = \beta_{\pm} q / [(a^2 - 1)q^2 + 1]$ ,  $Y = \beta/2 - a_c^2 q X$  and  $Z = q(a^2 - a_c^2) - 1/q$ . Again, we can read off the coefficients  $a_i$ ,  $b_i$  and  $c_i$  and then use Eq. (14) to find the coefficients

$$y_{C,0} = 1, \quad (38a)$$

$$y_{C,1} = MY \left( 1 + \frac{1}{v^2} \right), \quad (38b)$$

$$y_{C,2} = M^2 \left[ -X^2 \left( 1 + \frac{1}{v^2} \right) + Y^2 \left( 2 + \frac{6}{v^2} \right) + \frac{1}{8} \right], \quad (38c)$$

$$y_{C,3} = M^3 \left[ \frac{Z}{2} X^3 \left( 1 + \frac{1}{v^2} \right) - X^2 Y \left( \frac{9}{2} + \frac{12}{v^2} + \frac{3}{2v^4} \right) + Y^3 \left( \frac{9}{2} + \frac{49}{2v^2} + \frac{15}{2v^4} - \frac{1}{2v^6} \right) + Y \left( \frac{1}{2} + \frac{1}{2v^2} \right) \right]. \quad (38d)$$

Substituting them into Eq. (16), the deflection angle in the four-dimensional CEB spacetime is obtained as

$$\Delta\phi_C = \sum_{m=0}^{\infty} y_{C,m} \frac{I_m(\theta_s, \theta_d)}{b^m}. \quad (39)$$

To be complete, we also give the infinite source and detector distance limit of this deflection

$$\begin{aligned} \Delta\phi_C = & \pi + 2Y \left( 1 + \frac{1}{v^2} \right) \frac{M}{b} + \frac{\pi}{2} \left[ -X^2 \left( 1 + \frac{1}{v^2} \right) + Y^2 \left( 2 + \frac{6}{v^2} \right) + \frac{1}{8} \right] \frac{M^2}{b^2} \\ & + \frac{4}{3} \left[ \frac{Z}{2} X^3 \left( 1 + \frac{1}{v^2} \right) - X^2 Y \left( \frac{9}{2} + \frac{12}{v^2} + \frac{3}{2v^4} \right) \right. \\ & \left. + Y^3 \left( \frac{9}{2} + \frac{49}{2v^2} + \frac{15}{2v^4} - \frac{1}{2v^6} \right) + Y \left( \frac{1}{2} + \frac{1}{2v^2} \right) \right] \frac{M^3}{b^3} + \mathcal{O} \left( \frac{M}{b} \right)^4. \end{aligned} \quad (40)$$

In Fig. 4 (a), a comparison of the truncated deflection angle  $\Delta\phi_{C,\bar{m}}$  and the numerical result is made for a range of  $b$ . It is seen that again, as in the previous two cases, the series result approaches the true physical value exponentially as the order increases. The difference between  $\Delta\phi_{C,\bar{10}}$  and  $\Delta\phi_{C,\text{num}}$  is only about  $10^{-6}$  even for  $b = 7M$  at which point the deflection is roughly 0.4. In Fig. 4 (b)-(d), the dependence of  $\Delta\phi_C$  on the spacetime charge  $q$ , dilaton coupling constant  $a$  and parameter  $\beta$  are plotted. It is seen that as  $q$  or  $a$  increases, the

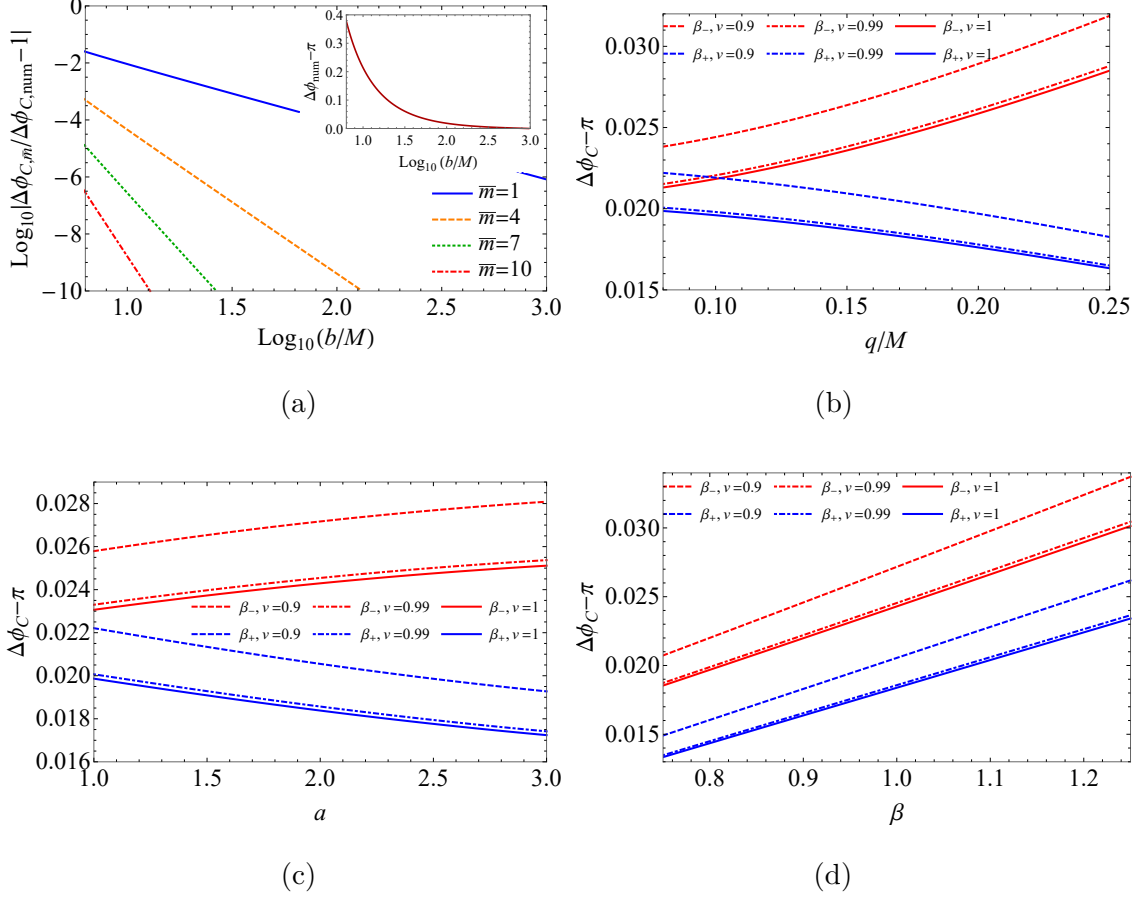


FIG. 4: (a) Difference between the perturbative  $\Delta\phi_{C,\bar{m}}$  and the numerical result  $\Delta\phi_{C,\text{num}}$  as a function of  $b/M$  from  $7$  to  $10^3$ . The inset shows the deflection angle itself for this range of  $b$ . Other parameters used are  $q = M/6$ ,  $\beta = 1$ ,  $a = 2$ ,  $v = 1 - 10^{-2}$ ,  $r_s = r_d = 10^6 M$  and we only showed for  $\beta_+$ .  $\Delta\phi_C$  as a function of  $q/M$  from  $1/12$  to  $1/4$  (b), of  $a$  from  $1$  to  $3$  (c), and of  $\beta$  from  $3/4$  to  $5/4$  (d). We plot for  $b = 100M$  and three values of  $v = 1, 0.99, 0.9$  in (b)-(d). Other parameters are the same as in (a).

deflection angles with branch  $\beta_+$  (or  $\beta_-$ ) will increase (or decrease) monotonically. On the other hand, both the deflections with branch  $\beta_+$  and  $\beta_-$  will increase as the parameter  $\beta$  increases. Finally in all these plots, the deflection angles will decrease as the signal velocity  $v$  increases, as expected.

In addition to the  $n=4$  case, to examine the power of the perturbative method, we also investigated the deflection in the CEB spacetime with arbitrary spacetime dimension.

Carrying out the asymptotic expansion of the metric (35) with general  $n$ , it is found that

$$A(r) = 1 + \frac{2Y}{n-3} \frac{M}{r^{n-3}} + (a_c^2 X^2 + 2Y^2) \frac{M^2}{r^{2n-6}} - \left( \frac{a_c^2 Z}{3} X^3 + 2a_c^2 X^2 Y + \frac{4}{3} Y^3 - \frac{1}{6} Y \right) \frac{M^3}{r^{3n-9}} + \mathcal{O}(r)^{4(3-n)}, \quad (41a)$$

$$B(r) = 1 - 2Y \frac{M}{r^{n-3}} - \left[ \frac{a_c^2 X^2}{n-3} - \frac{2Y^2}{(n-3)^2} + \frac{n-4}{4} \right] \frac{M^2}{r^{2n-6}} + \left[ \frac{a_c^2 Z X^3}{3(n-3)} - \frac{2a_c^2 X^2 Y^2}{(n-3)^2} + \frac{4Y^3}{3(n-3)^3} + \frac{n-9}{6(n-3)^2} \right] \frac{M^3}{r^{3n-9}} + \mathcal{O}(r)^{4(3-n)}, \quad (41b)$$

$$\frac{C(r)}{r^2} = 1 - 2Y \frac{M}{r^{n-3}} - \left[ \frac{a_c^2 X^2}{n-3} - \frac{2Y^2}{(n-3)^2} - \frac{1}{4(n-3)} \right] \frac{M^2}{r^{2n-6}} + \left[ \frac{a_c^2 Z X^3}{3(n-3)} - \frac{2a_c^2 X^2 Y^2}{(n-3)^2} + \frac{4Y^3}{3(n-3)^3} - \frac{n-6}{6(n-3)^2} \right] \frac{M^3}{r^{3n-9}} + \mathcal{O}(r)^{4(3-n)}. \quad (41c)$$

Reading off the coefficients  $a_i$ ,  $b_i$  and  $c_i$  ( $i \in \mathbb{Z}$ ) and substituting into Eq. (14), it is found that only the  $m(n-3)$  ( $m \in \mathbb{Z}_{\geq}$ ) order coefficients  $y_{C,m(n-3)}$  are nonzero. The first few of them are

$$y'_{C,0} = 1, \quad (42a)$$

$$y'_{C,n-3} = MY \left( 1 + \frac{n-3}{v^2} \right), \quad (42b)$$

$$y'_{C,2n-6} = M^2 \left\{ -a_c^2 X^2 \left( 1 + \frac{n-3}{v^2} \right) + Y^2 \left[ 2 + \frac{6(n-3)}{v^2} + \frac{2(n-3)(n-4)}{v^4} \right] + \frac{1}{8} \right\}, \quad (42c)$$

$$y'_{C,3n-9} = M^3 \left\{ \frac{a_c^2 Z}{2} X^3 \left( 1 + \frac{n-3}{v^2} \right) - a_c^2 X^2 Y \left[ \frac{9}{2} + \frac{12(n-3)}{v^2} + \frac{3(n-3)(3n-11)}{2v^4} \right] + Y^3 \left[ \frac{9}{2} + \frac{49(n-3)}{2v^2} + \frac{15(n-3)(3n-11)}{2v^4} + \frac{(n-3)(3n-11)(3n-13)}{2v^6} \right] + Y \left( \frac{1}{2} + \frac{n-3}{2v^2} \right) \right\}. \quad (42d)$$

The deflection angle for general dimensional CEB spacetime is then found using Eq. (16) as

$$\Delta\phi'_C = \sum_{m=0}^{\infty} y'_{C,m(n-3)} \frac{I_{m(n-3)}(\theta_s, \theta_d)}{b^{m(n-3)}}. \quad (43)$$

From Eq. (43) we immediately recognize that the first nontrivial order of the deflection is about  $y'_{C,n-3}/b^{n-3}$ . Since  $n > 4$  and  $b$  is usually larger than  $M$  which characterize the spacetime, clearly the deflection angle will decrease roughly by a factor of  $M/b$  when  $n$  increases by 1. In other words, the size of the deflection angle decreases roughly as a geometrical series with  $M/b$  as the common ratio as  $n$  increases. In Fig. 5, we plot the

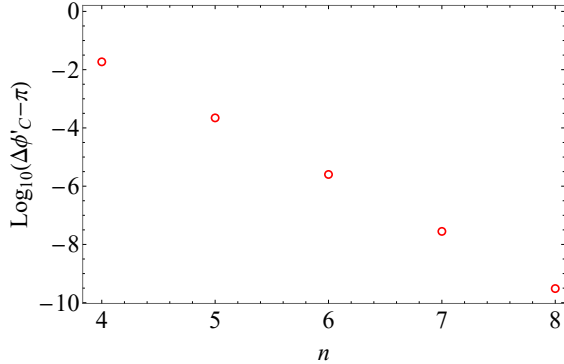


FIG. 5: The deflection  $\Delta\phi'_C - \pi$  as a function of the spacetime dimension  $n$ . The parameters are the same as in Fig. 4 (a) and we chose  $b = 100M$ .

deflection angle (43) for  $n = 4, 5, 6, 7, 8$  for  $b = 100M$  and infinite  $r_{s,d}$ . Other parameters used in this figure are the same as in Fig. 4 (a). Clearly, as  $n$  increases by 1 each time, the deflection decrease roughly by two orders of magnitude, which is exactly the  $M/b$  value we took in the plot. We note that the dependence of  $\Delta\phi_C$  on  $n$  at the leading order as  $\mathcal{O}(M/b)^{n-3}$  is also observed in Ref. [46].

Here, one more point we want to emphasize is that if  $r_{s,d}$  are finite, then their correction through  $I_0(\theta_s, \theta_d)$  to  $\Delta\phi'_C$  will be much more important in higher dimensional spacetime than  $n = 4$ . The reason is that the leading order finite distance correction, as revealed by Eq. (17), is always  $-b/r_{s,d}$  regardless of the dimension  $n$ . However, the first non-trivial order due to the impact parameter is proportional to  $M^{n-3}/b^{n-3}$  which decrease rapidly as  $n$  increases. Therefore, the higher the spacetime dimension, the more important the finite distance effect of the source and detector.

#### IV. EXTENSION TO ASYMPTOTICALLY NON-MINKOWSKI SPACETIMES

In this section, we show that the perturbative method can be extended to spacetimes that are asymptotically non-Minkowski to find the deflection angle in them. We will take the BH solution in a nonlinear electro-dynamical scalar theory as an example. Note that although this spacetime is asymptotically non-Minkowski, it is still asymptotically flat.

To extend the perturbative method to the asymptotically non-Minkowski case, we will not explicitly repeat all the calculations but only point out the steps that are different from the original derivation in Sec. II. We will assume that the metric functions have asymptotic

expansions of the form

$$A(r) = \sum_{n=0} \frac{a_n}{r^n}, \quad B(r) = \sum_{n=0} \frac{b_n}{r^n}, \quad \frac{C(r)}{r^2} = \sum_{n=0} \frac{c_n}{r^n}, \quad (44)$$

where  $a_0$ ,  $b_0$  and  $c_0$  are not all equal to one.

To use our method to this kind of spacetimes, we should first derive new relation between  $(E, L)$  and  $(v, b)$  from Eq. (3). For a static observer at infinity, its four-velocity is given by  $Z^\mu = (1/\sqrt{a_0}, 0, 0, 0)$ . A particle with four-velocity  $U^\mu = (dt/d\tau, dr/d\tau, 0, d\phi/d\tau)$  then will be detected to have velocity

$$v^\mu = h_\nu^\mu U^\nu / \gamma = \frac{1}{\gamma} \left( 0, \frac{dr}{d\tau}, 0, \frac{d\phi}{d\tau} \right), \quad (45)$$

in this observer's inertial coordinate system. Here  $h_{\mu\nu} = g_{\mu\nu} + Z_\mu Z_\nu$  is the induced metric and

$$\gamma = -Z^\mu U_\mu = \sqrt{a_0} dt/d\tau \quad (46)$$

is the  $\gamma$  factor. The asymptotic velocity  $v$  of this signal is defined as the norm of  $v^\mu$

$$v^2 = h_{\mu\nu} v^\mu v^\nu \Big|_{r \rightarrow \infty} = \frac{1}{\gamma^2} \left[ b_0 \left( \frac{dr}{d\tau} \right)^2 + c_0 r^2 \left( \frac{d\phi}{d\tau} \right)^2 \right]. \quad (47)$$

The proper time of the signal at infinity satisfies the following relation

$$-d\tau^2 = ds^2 = -a_0 dt^2 + b_0 dr^2 + c_0 r^2 d\phi^2 \quad (48)$$

$$= -a_0 dt^2 + \gamma^2 v^2 d\tau^2 \quad (49)$$

$$= -a_0 (1 - v^2) dt^2, \quad (50)$$

where in the second and third step Eqs. (47) and (46) are used respectively. From this, we are able to obtain that for the static observer at infinity

$$\frac{dt}{d\tau} = \frac{1}{\sqrt{a_0(1-v^2)}}, \quad \gamma = \frac{1}{\sqrt{1-v^2}}. \quad (51)$$

Combining this with Eq. (3a), we found the new relation between  $E$  and  $v$

$$E = A(r) \frac{dt}{d\tau} \Big|_{r \rightarrow \infty} = \frac{\sqrt{a_0}}{\sqrt{1-v^2}}. \quad (52)$$

To get a proper definition of the impact parameter  $b$  in this case, we recall that its geometric definition is the distance from the lens center to the straight asymptotic line of the trajectory, and therefore

$$b \equiv \sin \delta \cdot d_{LO} \Big|_{r \rightarrow \infty} \approx \frac{|\mathbf{v}_\phi|}{v} d_{OL} \Big|_{r \rightarrow \infty} = \frac{v^\phi d_{OL}}{v} \Big|_{r \rightarrow \infty}. \quad (53)$$

Here  $\delta$  is the angle by the three velocity  $\mathbf{v}$  itself and its  $\phi$ -component  $\mathbf{v}_\phi$ , and  $d_{OL}$  is the distance from the observer to the lens. Using (45) for  $v^\phi$ , Eq. (51) for  $\gamma$  and  $d_{OL} = \sqrt{c_0}r$ , this becomes

$$b = c_0 r^2 \frac{\sqrt{1-v^2}}{v} \frac{d\phi}{d\tau}. \quad (54)$$

Finally substituting this equation into Eq. (3b), we obtain the new relation between  $L$  and  $(b, v)$  as

$$L = C \frac{d\phi}{d\tau} \Big|_{r \rightarrow \infty} = \frac{bv}{\sqrt{1-v^2}}. \quad (55)$$

It is seen that by comparing to Eq. (6) the relation between  $L$  and  $(b, v)$  is not affected by the asymptotically non-Minkowski metric.

Corresponding to the new relations (52) and (55), the function  $p(x)$  in Eq. (8) should also be revised to

$$\frac{1}{b} = \frac{1}{\sqrt{a_0}} \frac{\sqrt{E^2 - a_0 \kappa}}{\sqrt{E^2 - \kappa A(r_0)}} \sqrt{\frac{A(r_0)}{C(r_0)}} \equiv p\left(\frac{1}{r_0}\right). \quad (56)$$

With these changes, formally  $\Delta\phi$  still take the form of Eq. (16), i.e.,

$$\Delta\phi = \sum_{n=0}^{\infty} y_n \frac{I_n(\theta_s, \theta_d)}{b^n} \quad (57)$$

but with the following revised series coefficients

$$y_0 = \sqrt{\frac{b_0}{c_0}}, \quad (58a)$$

$$y_1 = \sqrt{\frac{b_0}{c_0}} \left( \frac{b_1 \sqrt{c_0}}{2b_0} \right) \left( 1 - \frac{a_1 b_0}{a_0 b_1} \frac{1}{v^2} \right), \quad (58b)$$

$$y_2 = \sqrt{\frac{b_0}{c_0}} \left( \frac{b_1 \sqrt{c_0}}{2b_0} \right)^2 \left[ \frac{2b_0^2 c_2}{b_1^2 c_0} - \frac{b_0^2 c_1^2}{2b_1^2 c_0^2} + \frac{b_0 c_1}{b_1 c_0} + \frac{2b_0 b_2}{b_1^2} - \frac{1}{2} \right. \\ \left. - \left( \frac{2a_1 b_0^2 c_1}{a_0 b_1^2 c_0} + \frac{4a_2 b_0^2}{a_0 b_1^2} - \frac{4a_1^2 b_0^2}{a_0^2 b_1^2} + \frac{2a_1 b_0}{a_0 b_1} \right) \frac{1}{v^2} \right]. \quad (58c)$$

One can easily check that this system reduces to Eq. (14) when  $a_0 = b_0 = c_0 = 1$ . In Eq. (57), the  $I_n$  are still given by Eq. (A2) while the  $\theta_s$  and  $\theta_d$  are still given by Eq. (12) with new function  $p(x)$  given by Eq. (56).

## Application to NES theory

The metric functions of a nonlinear electrodynamical massless scalar theory are given by [47]

$$A(r) = \frac{1}{B(r)} = -\frac{1}{\sqrt{2}\beta} \left[ \frac{r-r_1}{r-r_2} \right]^\nu, \quad C(r) = \beta^2(r-r_1)(r-r_2) \left[ \frac{r-r_2}{r-r_1} \right]^\nu, \quad (59)$$

where  $\beta = q_m - \sqrt{2}$  is the electrodynamical strength parameter with  $q_m$  being a non-negative magnetic charge. Since  $\beta$  has to be negative in order for the temporal metric function to have the correct sign, this effectively set a range for  $q_m$  to be  $0 \leq q_m < \sqrt{2}$ . The parameter  $\nu \in (0, 1)$  in Eq. (59) characterizes the strength of the scalar field.  $r_1 > r_2$  are two constants appearing in the NES theory solution, and it was shown that  $r = r_1$  is the location of the event horizon of the BH in this spacetime [47]. Moreover, unlike event horizons of Schwarzschild or RN BHs, this event horizon is a true physical singularity of the spacetime. Note that this spacetime reduces to the Janis-Newmann-Winicour spacetime in the limit  $\beta \rightarrow -\sqrt{2}$  and  $r_1 \rightarrow -r_2$  [47].

The metric (59) can be expanded asymptotically as

$$A(r) = -\frac{1}{\sqrt{2}\beta} \left[ 1 - \frac{\nu(r_1 - r_2)}{r} + \frac{\nu(r_1 - r_2)(\nu r_1 - \nu r_2 - r_1 - r_2)}{2} \frac{1}{r^2} \right] + \mathcal{O}(r)^{-3}, \quad (60a)$$

$$B(r) = -\sqrt{2}\beta \left[ 1 + \frac{\nu(r_1 - r_2)}{r} + \frac{\nu(r_1 - r_2)(\nu r_1 - \nu r_2 + r_1 + r_2)}{2} \frac{1}{r^2} \right] + \mathcal{O}(r)^{-3}, \quad (60b)$$

$$\begin{aligned} \frac{C(r)}{r^2} = & \beta^2 \left\{ 1 + [(\nu - 1)r_1 - (\nu + 1)r_2] \frac{1}{r} \right. \\ & \left. + \left[ -(\nu^2 - 1)r_2 r_1 + \frac{1}{2}\nu(\nu - 1)r_1^2 + \frac{1}{2}\nu(\nu + 1)r_2^2 \right] \frac{1}{r^2} \right\} + \mathcal{O}(r)^{-3}. \end{aligned} \quad (60c)$$

From this, one can immediately see that at infinity

$$a_0 = \frac{1}{b_0} = -\frac{1}{\sqrt{2}\beta}, \quad c_0 = \beta^2. \quad (61)$$

If  $\beta$  were  $-\sqrt{2}$ , i.e.,  $q_m$  were zero, then a scaling  $t' = t/\sqrt{2}$ ,  $r' = \sqrt{2}r$  will be able to transform the NES solution to an asymptotically Minkowski spacetime, which we will not be interested in this work. When  $q_m$  is nonzero and  $\beta \neq -\sqrt{2}$  however, we see that the spacetime is asymptotically non-Minkowski.

Reading off the coefficients  $a_i$ ,  $b_i$  and  $c_i$  from Eq. (60) and substituting into Eq. (58), we are able to obtain

$$y_{N,0} = \frac{\sqrt[4]{2}}{\sqrt{-\beta}}, \quad (62a)$$

$$y_{N,1} = \frac{\sqrt[4]{2}}{\sqrt{-\beta}}(-\beta M) \left(1 + \frac{1}{v^2}\right), \quad (62b)$$

$$y_{N,2} = \frac{\sqrt[4]{2}}{\sqrt{-\beta}}(-\beta M)^2 \left(2 - \frac{1}{2\nu^2} + \frac{6}{v^2}\right), \quad (62c)$$

where we have defined an effective ADM mass  $M = \nu(r_1 - r_2)/2$  of the system, inspired by the first order of Eq. (60a). Substituting these into Eq. (57), we are able to obtain the deflection angle  $\Delta\phi_N$  in this NES spacetime

$$\Delta\phi_N = \sum_{n=0}^{\infty} y_{N,n} \frac{I_n(\theta_s, \theta_d)}{b^n}, \quad (63)$$

where  $I_n$  are still given by Eq. (A2) while the  $\theta_s$  and  $\theta_d$  are still given by Eq. (12) with new function  $p(x)$  given by Eq. (56) for the metric (59). From the coefficients  $y_{N,n}$  in Eq. (62) and the higher order ones, we can tell that in order for Eq. (63) to converge, the ratio of the adjacent terms in this series has to be smaller than one. When  $\nu$  is small, inspecting Eq. (62) shows that this condition effectively becomes  $-\beta M/(\nu^2 b) \lesssim 1$ , i.e.,  $\nu > \sqrt{-\beta M/b} = \sqrt{-(q_m - \sqrt{2})M/b}$ , which can be thought as a condition for the deflection angle (63) to be valid. In the  $r_s, r_d \rightarrow \infty$  limit,  $\Delta\phi_N$  becomes much simpler

$$\Delta\phi_N = \frac{\sqrt[4]{2}}{\sqrt{-\beta}} \left[ \pi - 2\beta M \left(1 + \frac{1}{v^2}\right) \frac{1}{b} + \pi\beta^2 M^2 \left(1 - \frac{1}{\nu^2} + \frac{3}{v^2}\right) \frac{1}{b^2} \right] + \mathcal{O}\left(\frac{M}{b}\right)^3. \quad (64)$$

Similar to the cases in Sec. III, we can define a truncated partial sum  $\Delta\phi_{N,\bar{m}}$  and compare it with the numerical integration result, as shown in Fig. 6(a). Again, this shows that the perturbative result works very well, even for smaller  $b$  at which the deflection angle is not that small anymore. While in Fig. 6 (b), we plot the dependence of  $\Delta\phi_N$  on its parameters  $0 \leq q_m < \sqrt{2}$  and  $\sqrt{(\sqrt{2} - q_m)M/b} < \nu < 1$  for  $b = 100M$ . It is seen that for a fixed  $\nu$ , as the magnetic charge increases, the deflection angle decreases. This is qualitatively similar to the effect of electrical charge in some charged spacetimes, such as the RN spacetime [31, 40]. For fixed  $q_m$  however, as  $\nu$  increases, the deflection angle keeps increasing, although the increase rate becomes very small after about 0.2.

Theoretically, we observe from Eq. (58a) (or Eq. (64) in the NES spacetime) one of the most fundamental feature for geodesic motion in an asymptotically non-Minkowski spacetime: the deflection angle at leading order is not  $\pi$  anymore. Since  $-\sqrt{2} < \beta < 0$ , using Eqs. (58a) and (60), we have  $y_0 = \sqrt{b_0/c_0} = \sqrt[4]{2}/\sqrt{-\beta} > 1$ . Combining with  $I_0(r_i \rightarrow \infty) = \pi/2$ , this means that the deflection angle with an infinite  $b$  in this spacetime is larger than  $\pi$ .

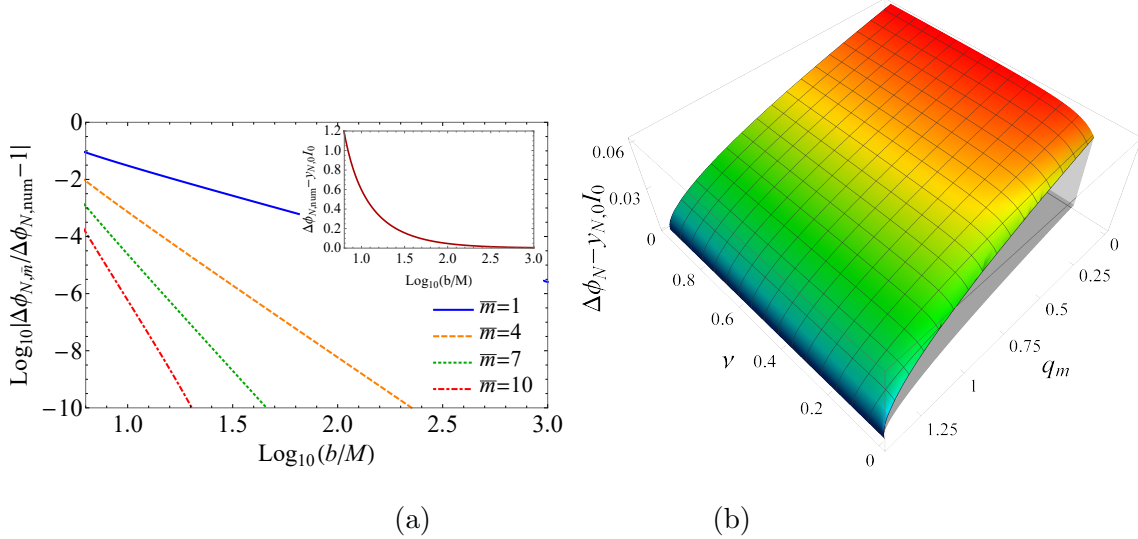


FIG. 6: (a) Difference between the perturbative  $\Delta\phi_{N,\bar{m}}$  and the numerical result  $\Delta\phi_{N,\text{num}}$  as a function of  $b/M$  from 7 to  $10^3$ . The inset shows the deflection angle itself for this range of  $b$ . Other parameters used are  $q_m = 1/2$ ,  $\nu = 1 - 10^{-2}$ ,  $r_s = r_d = 10^6 M$  and  $\nu = 1/2$ ,  $r_1 = -r_2 = M/\nu$ . (b)  $\Delta\phi_N$  as a function of  $q_m$  and  $\nu$  for  $b = 100M$ . Other parameters are the same as in (a).

The above feature for asymptotically non-Minkowski spacetime actually can be understood in the following geometrical way. First we notice that asymptotically, the metric for the equatorial plane of the spacetime (59) can be approximated by

$$ds^2 = -a_0 dt^2 + b_0 dr^2 + c_0 r^2 d\phi^2, \quad b_0 > c_0 > 0. \quad (65)$$

Now consider a cone structure

$$\frac{z^2}{r^2} = \frac{b_0}{c_0} - 1 > 0 \quad (66)$$

living in a spacetime with line element

$$ds^2 = -a_0 dt^2 + c_0 [dr^2 + r^2 d\phi^2 + dz^2], \quad (67)$$

then substituting Eq. (66) into Eq. (67) one sees that the induced metric of the cone will be exactly the same as Eq. (65). Therefore, any geodesics on the cone is also a geodesic on the equatorial plane after simple projection  $(r, \phi, z) \rightarrow (r, \phi)$ , as illustrated in Fig. 7 (left).

On the other hand, it is known that a cone, after cut along its generatrix, is flat, and therefore any geodesic on it is necessarily a straight line. However, when wrapped into a cone and projected onto the equatorial plane, apparently its deflection angle at the leading

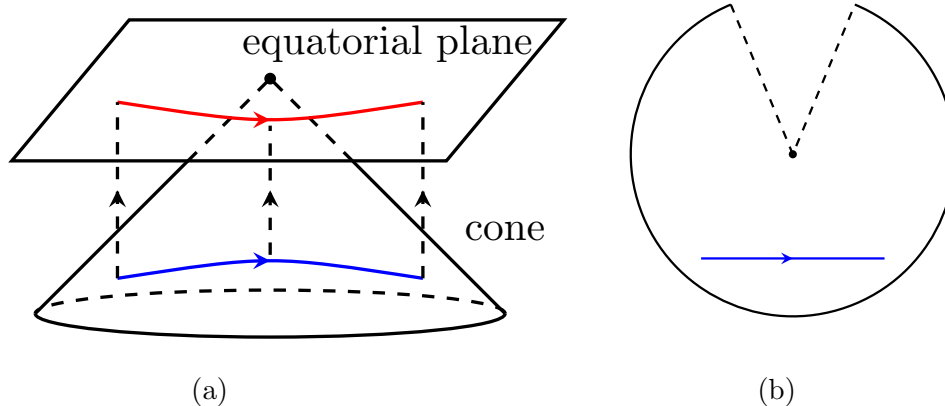


FIG. 7: (a) The trajectory in the equatorial plane and the cone which project to the plane. (b) The unwrapped cone and the geodesic on its surface.

order will be larger than  $\pi$ , as seen from Fig. 7 (right). Therefore this simple geometric analogy explains the result in the leading order of Eq. (64).

## V. CONCLUSIONS

In this work, we used a perturbative technique to compute the deflection of null and timelike signals in arbitrary static and spherically symmetric spacetimes in the weak field limit. The technique naturally takes into account the finite distance effect of the source and observer. The resultant deflection angle takes a (quasi-)power series form of  $M/b$ , which can be converted to a dual-power series form of  $M/b$  and  $b/r_{s,d}$ . We then applied this method to the extended Einstein-Maxwell spacetime, the Born-Infeld gravity and the charged Ellis-Bronnikov spacetime. It is shown by comparison to numerical method that the perturbative deflection angle works extremely well. In particular, in the last spacetime, we also illustrated that the perturbative method can be applied to spacetime with arbitrary dimension without any difficulty. The deflection at the leading order is found to decrease as  $\mathcal{O}(M/b)^{n-3}$  as the dimension  $n$  increases.

In the second part, we extended the perturbative method to the asymptotically non-Minkowski spacetimes and applied the result to a nonlinear electro-dynamical scalar theory. It is shown that one fundamental feature of this kind of spacetimes is that the deflection angle at the leading order is not  $\pi$  anymore. We provided a simple geometrical understanding of this feature. In each of the above spacetimes, we studied the effects of the spacetime

parameters and the signal velocity on the deflection angle.

Regarding possible further development of this work, there are at least the following possibilities. The first is to use the deflection angles found in these spacetimes to study the gravitational lensing effect, including the time delay between lensed images. The second is to further develop the method to handle other types of spacetimes such as those with logarithmic asymptotic expansions [48, 49]. We are currently working along these directions.

### Acknowledgments

We thank Haotian Liu for helping with the schematic diagrams. This work is supported by (China-Ukraine IGSCP-12).

### Appendix A: Integration formulas

This integral (15) can be carried out using a change of variable  $u = \sin \xi$  to find an elementary expression for even and odd non-negative  $m$  respectively [50]

$$I_m(\theta_s, \theta_d) = \left[ \int_{\theta_s}^{\pi/2} + \int_{\theta_d}^{\pi/2} \right] \sin^m \xi d\xi \quad (m \in \mathbb{Z}_{\geq}) \quad (\text{A1})$$

$$= \sum_{i=s,d} \frac{(m-1)!!}{m!!} \times \begin{cases} \left( \frac{\pi}{2} - \theta_i + \cos \theta_i \sum_{j=1}^{\lfloor \frac{m-1}{2} \rfloor} \frac{(2j-2)!!}{(2j-1)!!} \sin^{2j-1} \theta_i \right), & m \text{ is even,} \\ \cos \theta_i \left( 1 + \sum_{j=1}^{\lfloor \frac{m-1}{2} \rfloor} \frac{(2j-1)!!}{(2j)!!} \sin^{2j} \theta_i \right), & m \text{ is odd.} \end{cases} \quad (\text{A2})$$

To be explicit, the first few  $I_n$ 's are

$$I_0(\theta_i) = \frac{\pi}{2} - \theta_i, \quad (\text{A3a})$$

$$I_1(\theta_i) = \cos(\theta_i), \quad (\text{A3b})$$

$$I_2(\theta_i) = \frac{1}{4} (\pi - 2\theta_i + \sin(2\theta_i)), \quad (\text{A3c})$$

$$I_3(\theta_i) = \frac{1}{12} (9 \cos(\theta_i) - \cos(3\theta_i)). \quad (\text{A3d})$$

When  $\theta_s = \theta_d = 0$  as in the infinite distance case, this can be further simplified to

$$I_m(0, 0) = \frac{(m-1)!!}{m!!} \times \begin{cases} \pi, & m \text{ is even,} \\ 2, & m \text{ is odd.} \end{cases} \quad (\text{A4})$$

For the finite distance case however,  $b/r_{s,d}$  ( $i = s, d$ ) is only small but nonzero. In this case, we can make an expansion of  $I_n$  for small  $b/r_{s,d}$  too by first using Eq. (12) to expand  $\theta_i$  in this limit. To the first few orders, we have

$$\theta_i = \frac{b}{r_i} - \frac{b}{r_i^2} \left( \frac{c_1}{2} - \frac{a_1}{2v^2} \right) + \frac{b^3}{6r_i^3} + \frac{b}{4r_i^3} \left( \frac{3c_1^2 - 4c_2}{2} - \frac{2a_1^2 - 2a_2 + a_1c_1}{v^2} + \frac{2a_1^2}{2v^4} \right) + \mathcal{O}(\varepsilon)^4 \quad (\text{A5})$$

where  $\varepsilon$  stands for either the infinitesimal  $b/r_i$  or  $M/b$ . Substituting this into the first few  $I_n$  in Eq. (A3), their expansions becomes

$$I_0 = \frac{\pi}{2} - \frac{b}{r_i} + \frac{b}{r_i^2} \left( \frac{c_1}{2} - \frac{a_1}{2v^2} \right) - \frac{b^3}{6r_i^3} - \frac{b}{4r_i^3} \left( \frac{3c_1^2 - 4c_2}{2} - \frac{2a_1^2 - 2a_2 + a_1c_1}{v^2} + \frac{2a_1^2}{2v^4} \right) + \mathcal{O}(\varepsilon)^4, \quad (\text{A6a})$$

$$I_1 = 1 - \frac{b^2}{2r_i^2} - \frac{b^2(a_1 - c_1v^2)}{2v^2r_i^3} + \mathcal{O}(\varepsilon)^3, \quad (\text{A6b})$$

$$I_2 = \frac{\pi}{4} - \frac{b^3}{3r_i^3} + \mathcal{O}(\varepsilon)^4, \quad (\text{A6c})$$

$$I_3 = \frac{2}{3} + \mathcal{O}(\varepsilon)^4. \quad (\text{A6d})$$

- 
- [1] F. W. Dyson, A. S. Eddington and C. Davidson, *Phil. Trans. Roy. Soc. Lond. A* **220**, 291-333 (1920) doi:10.1098/rsta.1920.0009
- [2] S. Mao and B. Paczynski, *Astrophys. J. Lett.* **374**, L37-L40 (1991) doi:10.1086/186066
- [3] C. Alcock *et al.* [Supernova Cosmology Project], *Nature* **365**, 621-623 (1993) doi:10.1038/365621a0 [arXiv:astro-ph/9309052 [astro-ph]].
- [4] H. Hoekstra, M. Franx, K. Kuijken, R. G. Carlberg, H. K. C. Yee, H. Lin, S. L. Morris, P. B. Hall, D. R. Patton and M. Sawicki, *et al.* *Astrophys. J. Lett.* **548**, L5 (2001) doi:10.1086/318917 [arXiv:astro-ph/0012169 [astro-ph]].
- [5] M. E. Gray, A. N. Taylor, K. Meisenheimer, S. Dye, C. Wolf and E. Thommes, *Astrophys. J.* **568**, 141 (2002) doi:10.1086/338763 [arXiv:astro-ph/0111288 [astro-ph]].
- [6] H. Hoekstra and B. Jain, *Ann. Rev. Nucl. Part. Sci.* **58**, 99-123 (2008) doi:10.1146/annurev.nucl.58.110707.171151 [arXiv:0805.0139 [astro-ph]].
- [7] A. Joyce, L. Lombriser and F. Schmidt, *Ann. Rev. Nucl. Part. Sci.* **66**, 95-122 (2016) doi:10.1146/annurev-nucl-102115-044553 [arXiv:1601.06133 [astro-ph.CO]].

- [8] B. P. Abbott *et al.* [LIGO Scientific and Virgo], *Phys. Rev. Lett.* **116**, no.6, 061102 (2016) doi:10.1103/PhysRevLett.116.061102 [arXiv:1602.03837 [gr-qc]].
- [9] K. Akiyama *et al.* [Event Horizon Telescope], *Astrophys. J. Lett.* **875**, L1 (2019) doi:10.3847/2041-8213/ab0ec7 [arXiv:1906.11238 [astro-ph.GA]].
- [10] K. Akiyama *et al.* [Event Horizon Telescope], *Astrophys. J. Lett.* **875**, no.1, L6 (2019) doi:10.3847/2041-8213/ab1141 [arXiv:1906.11243 [astro-ph.GA]].
- [11] K. Akiyama *et al.* [Event Horizon Telescope], *Astrophys. J. Lett.* **930**, no.2, L12 (2022) doi:10.3847/2041-8213/ac6674
- [12] V. F. Hess, *Phys. Z.* **13**, 1084-1091 (1912)
- [13] K. Hirata *et al.* [Kamiokande-II], *Phys. Rev. Lett.* **58**, 1490-1493 (1987) doi:10.1103/PhysRevLett.58.1490
- [14] R. M. Bionta, G. Blewitt, C. B. Bratton, D. Casper, A. Ciocio, R. Claus, B. Cortez, M. Crouch, S. T. Dye and S. Errede, *et al.* *Phys. Rev. Lett.* **58**, 1494 (1987) doi:10.1103/PhysRevLett.58.1494
- [15] W. Baade and F. Zwicky, *Proc. Nat. Acad. Sci.* **20**, no.5, 254-259 (1934) doi:10.1073/pnas.20.5.254
- [16] W. Baade and F. Zwicky, *Phys. Rev.* **46**, 76 (1934)
- [17] B. T. Cleveland, T. Daily, R. Davis, Jr., J. R. Distel, K. Lande, C. K. Lee, P. S. Wildenhain and J. Ullman, *Astrophys. J.* **496**, 505-526 (1998) doi:10.1086/305343
- [18] Y. Fukuda *et al.* [Super-Kamiokande], *Phys. Rev. Lett.* **81**, 1562-1567 (1998) doi:10.1103/PhysRevLett.81.1562 [arXiv:hep-ex/9807003 [hep-ex]].
- [19] P. L. Kelly, S. A. Rodney, T. Treu, R. J. Foley, G. Brammer, K. B. Schmidt, A. Zitrin, A. Sonnenfeld, L. G. Strolger and O. Graur, *et al.* *Science* **347**, 1123 (2015) doi:10.1126/science.aaa3350 [arXiv:1411.6009 [astro-ph.CO]].
- [20] A. Goobar, R. Amanullah, S. R. Kulkarni, P. E. Nugent, J. Johansson, C. Steidel, D. Law, E. Mortsell, R. Quimby and N. Blagorodnova, *et al.* *Science* **356**, 291-295 (2017) doi:10.1126/science.aal2729 [arXiv:1611.00014 [astro-ph.CO]].
- [21] D. Glavan and C. Lin, *Phys. Rev. Lett.* **124**, no.8, 081301 (2020) doi:10.1103/PhysRevLett.124.081301 [arXiv:1905.03601 [gr-qc]].
- [22] G. W. Gibbons and M. C. Werner, *Class. Quant. Grav.* **25**, 235009 (2008) doi:10.1088/0264-9381/25/23/235009 [arXiv:0807.0854 [gr-qc]].

- [23] M. C. Werner, *Gen. Rel. Grav.* **44**, 3047-3057 (2012) doi:10.1007/s10714-012-1458-9 [arXiv:1205.3876 [gr-qc]].
- [24] T. Ono, A. Ishihara and H. Asada, *Phys. Rev. D* **96**, no.10, 104037 (2017) doi:10.1103/PhysRevD.96.104037 [arXiv:1704.05615 [gr-qc]].
- [25] Z. Li and J. Jia, *Eur. Phys. J. C* **80**, no.2, 157 (2020) doi:10.1140/epjc/s10052-020-7665-8 [arXiv:1912.05194 [gr-qc]].
- [26] Z. Li and J. Jia, *Phys. Rev. D* **104**, no.4, 044061 (2021) doi:10.1103/PhysRevD.104.044061 [arXiv:2108.05273 [gr-qc]].
- [27] A. Ishihara, Y. Suzuki, T. Ono, T. Kitamura and H. Asada, *Phys. Rev. D* **94**, no.8, 084015 (2016) doi:10.1103/PhysRevD.94.084015 [arXiv:1604.08308 [gr-qc]].
- [28] A. Ishihara, Y. Suzuki, T. Ono and H. Asada, *Phys. Rev. D* **95**, no.4, 044017 (2017) doi:10.1103/PhysRevD.95.044017 [arXiv:1612.04044 [gr-qc]].
- [29] Z. Li, Y. Duan and J. Jia, *Class. Quant. Grav.* **39**, 015002 (2022) doi:10.1088/1361-6382/ac38d0 [arXiv:2012.14226 [gr-qc]].
- [30] G. Crisnejo, E. Gallo and J. R. Villanueva, *Phys. Rev. D* **100**, no.4, 044006 (2019) doi:10.1103/PhysRevD.100.044006 [arXiv:1905.02125 [gr-qc]].
- [31] J. Jia, *Eur. Phys. J. C* **80**, no.3, 242 (2020) doi:10.1140/epjc/s10052-020-7796-y [arXiv:2001.02038 [gr-qc]].
- [32] K. Huang and J. Jia, *JCAP* **08**, 016 (2020) doi:10.1088/1475-7516/2020/08/016 [arXiv:2003.08250 [gr-qc]].
- [33] X. Xu, T. Jiang and J. Jia, *JCAP* **08**, 022 (2021) doi:10.1088/1475-7516/2021/08/022 [arXiv:2105.12413 [gr-qc]].
- [34] S. Zhou, M. Chen and J. Jia, [arXiv:2203.05415 [gr-qc]].
- [35] J. Jia and K. Huang, *Eur. Phys. J. C* **81**, no.3, 242 (2021) doi:10.1140/epjc/s10052-021-09026-7 [arXiv:2011.08084 [gr-qc]].
- [36] P. A. Cano and Á. Murcia, *Class. Quant. Grav.* **38**, no.7, 075014 (2021) doi:10.1088/1361-6382/abd923 [arXiv:2006.15149 [hep-th]].
- [37] S. Jana and S. Kar, *Phys. Rev. D* **92** (2015), 084004 doi:10.1103/PhysRevD.92.084004 [arXiv:1504.05842 [gr-qc]].
- [38] M. Nozawa, *Phys. Rev. D* **103**, no.2, 024004 (2021) doi:10.1103/PhysRevD.103.024004 [arXiv:2010.07560 [gr-qc]].

- [39] H. Liu and J. Jia, Chin. Phys. C **45**, no.8, 083102 (2021) doi:10.1088/1674-1137/ac03ab [arXiv:2006.03542 [gr-qc]].
- [40] X. Pang and J. Jia, Class. Quant. Grav. **36**, no.6, 065012 (2019) doi:10.1088/1361-6382/ab0512 [arXiv:1806.04719 [gr-qc]].
- [41] P. P. Avelino, Phys. Rev. D **85** (2012), 104053 doi:10.1103/PhysRevD.85.104053 [arXiv:1201.2544 [astro-ph.CO]].
- [42] P. Pani, V. Cardoso and T. Delsate, Phys. Rev. Lett. **107** (2011), 031101 doi:10.1103/PhysRevLett.107.031101 [arXiv:1106.3569 [gr-qc]].
- [43] Y. H. Sham, P. T. Leung and L. M. Lin, Phys. Rev. D **87** (2013) no.6, 061503 doi:10.1103/PhysRevD.87.061503 [arXiv:1304.0550 [gr-qc]].
- [44] P. P. Avelino, JCAP **11** (2012), 022 doi:10.1088/1475-7516/2012/11/022 [arXiv:1207.4730 [astro-ph.CO]].
- [45] J. Casanellas, P. Pani, I. Lopes and V. Cardoso, Astrophys. J. **745** (2012), 15 doi:10.1088/0004-637X/745/1/15 [arXiv:1109.0249 [astro-ph.SR]].
- [46] A. Belhaj, M. Benali, A. El Balali, H. El Moumni and S. E. Ennadifi, Class. Quant. Grav. **37**, no.21, 215004 (2020) doi:10.1088/1361-6382/abbaa9 [arXiv:2006.01078 [gr-qc]].
- [47] T. Tahamtan, Phys. Rev. D **101**, no.12, 124023 (2020) doi:10.1103/PhysRevD.101.124023 [arXiv:2006.02810 [gr-qc]].
- [48] M. H. Li and K. C. Yang, Phys. Rev. D **86**, 123015 (2012) doi:10.1103/PhysRevD.86.123015 [arXiv:1204.3178 [astro-ph.CO]].
- [49] H. X. Zhang, Y. Chen, T. C. Ma, P. Z. He and J. B. Deng, Chin. Phys. C **45**, no.5, 055103 (2021) doi:10.1088/1674-1137/abe84c [arXiv:2007.09408 [gr-qc]].
- [50] I.S.Gradshiteyn, and I.M.Ryzhik, *Table of Integrals, Series, and Products*, 8th ed. Academic Press (2014), p. 152.